Applied Mathematical Modelling 39 (2015) 764–775

Contents lists available at ScienceDirect

Applied Mathematical Modelling

journal homepage: www.elsevier.com/locate/apm

Dynamic modeling and simulation of a naphtha catalytic reforming reactor

Ignacio Elizalde [a,b,*], Jorge Ancheyta [b]

[a] Centro Mexicano para la Producción más Limpia, Instituto Politécnico Nacional, Ticomán, México, D.F. 07340, Mexico
[b] Escuela Superior de Ingeniería Química e Industrias Extractivas, Instituto Politécnico Nacional, Zacatenco, México D.F. 07738, Mexico

ARTICLE INFO

Article history:
Received 26 March 2013
Received in revised form 27 May 2014
Accepted 11 July 2014
Available online 19 July 2014

Keywords:
Dynamic modeling
Start-up
Perturbation
Reforming reactions

ABSTRACT

Modeling of reforming reactor was conducted by expressing the heat and mass balances under non-steady state conditions. Kinetic and thermodynamic parameters were taken from the literature. Simulation in steady-state and transient state was carried out by using Matlab software. It was determined that some compounds exhibit net increase in concentration such as low molecular weight paraffins, while other compounds undergo net disappearance. Depending on the compound the time to attain the pseudo-steady-state is different. Perturbation of feed temperature was also modeled. The time to achieve the quasi steady-state was obtained and when compared it with the start-up condition time they were almost similar under the conditions used in this study.

1. Introduction

Naphtha is a complex mixture of different families of hydrocarbons such as paraffins (alkanes), naphthenes (cycloalkanes) and aromatics containing 5–12 carbon atoms whose normal boiling point ranges between 30 and 200 °C. Catalytic reforming is a process that allows for upgrading low octane to high octane naphtha by means of a series of gas phase transformations of linear to branched and to cycloalkanes, and reaction of naphthenes to yield aromatics. The octane number is defined as the volume percent of iso-octane in blending with n-heptane that equals the performance of the naphtha being tested. As the concentration of aromatics and branched paraffins (reformate) increases as result of the reforming reactions so does the octane number and hence better performance of internal combustion engines is obtained.

A number of reactions occur during the catalytic reforming namely hydrocracking of paraffins, cyclization of straight alkanes, dehydrogenation/hydrogenation of naphthenes and aromatics, hydrodealkylation of substituted aromatics among the most important reactions [1]. As result of dehydrogenation reactions, hydrogen byproduct is obtained which is needed for hydrotreating and hydrocracking operations [2].

Modeling of naphtha catalytic reforming has been studied by employing different approaches. For instance Ancheyta et al. [2,3] have considered a number of reactions and complex network to properly simulate the reforming process, whereas Sotelo and Froment [4] have used a fundamental kinetic approach based on the single event concept that consists of modeling the huge number of reactions occurring in naphtha catalytic reforming in a reduced number of elementary steps while retaining details of each reaction such as pathway and intermediaries. While the fundamental approaches are not fully applied other approaches such as lumping kinetic procedure, that consist of grouping hydrocarbons of the same family with

* Corresponding author at: Centro Mexicano para la Producción más Limpia, Instituto Politécnico Nacional, Ticomán, México, D.F. 07340, Mexico. Tel.: +52 (55) 5729 6000x52602; fax: +52 (55) 5729 6000x52600.
E-mail address: ielizaldem@gmail.com (I. Elizalde).

http://dx.doi.org/10.1016/j.apm.2014.07.013
0307-904X/

Nomenclature

A_i	aromatic compound
A_r	cross-section reactor
C_A	molar concentration
C_{PG}	gas heat capacity at constant pressure
C_{PS}	solid heat capacity
E_a	activation energy
k	reaction rate constant
L	reactor length
MW_G	molecular weight of gas
N_i	naphthenic compound
P	pressure
P_i	paraffinic compound
P_0	reference pressure
R	universal gas constant
$\overline{r_A}$	mean reaction rate in the catalyst element weight
r_i	reaction rate
T	absolute temperature
T_∞	temperature length function at steady-state condition
t	time
u_G	linear gas velocity
w	catalyst weight
Y_i	molar concentration of i compound/total molar concentration
$Y_{i\infty}$	molar concentration of i compound at steady-state/total molar concentration at steady-state
z	axial position within the reactor

Subscripts

g	gas phase
i	ith-component
r	reactor
s	solid phase
0	inlet reactor condition or initial condition

Greek symbols

Δ	finite element
ε_G	gas holdup
ε_S	solid fraction
$\in_B$	bed porosity
ρ_B	bulk density
ω	acentric factor

the same number of carbons as one pseudo-component, are more versatile from an industrial point of view because the parameters to formulate the kinetics and reactor model can be obtained directly from experimental conditions and the kinetic model could work with acceptable accuracy. When modeling with the lumping approach it is better to use a greater number of pseudo-components due to closer agreement between experimental and simulations can be obtained although the identification of the huge number of feed components imposes severe restrictions for using such an approach.

Different catalytic processes are available for catalytic reforming such as: semi-regenerative, cyclic regeneration and continuous regeneration [2]. In semi-regenerative process the system consists of three or four in series reactors packed with catalyst particles [3]. Industrial reformers operate adiabatically, and because of the nature of reactions involved, the heat of endothermic reactions predominates over the heat of exothermic ones.

While kinetics of catalytic reforming reactions has been subject of continuous research, reactor modeling has received lesser attention. Important stages of reforming process such as start-up, shut-down, effect of transients due to changes in feed composition, and temperature increase due to catalyst deactivation are needed to be understood in order to improve the process and reactor design. According to Mederos et al. [5] capturing these features including the steady-state condition can be done by using a dynamic reactor model that also provides a more robust numerical solution.

In the present contribution the dynamic responses of start-of-run and perturbation by changing feed temperature of an adiabatic catalytic reactor where naphtha reforming is carried out was investigated by means of modeling. Kinetic

parameters and thermodynamic properties were taken from the literature. To solve the reactor model, which consists of a set of coupled differential equations, Matlab software was used.

2. The model

2.1. Assumptions

Some assumptions are necessary to establish in order to avoid excessive complexity, due to the reactor performance and lacking of some data. Such assumptions are:

- Negligible deactivation of catalyst, since cycle of catalyst life can be longer than 12 months while residence times are of the order of hours.
- Adiabatic operation, because industrial reactors are insulated with fiber glass or any other insulator which is placed in several layers on the external surface area of the reactor.
- Plug-flow pattern, because at the reaction conditions of pressure and temperature naphtha flows as gas through the reactor. Due to the reactor dimensions, mainly length, dispersion of matter is negligible as supported by a criterion reported elsewhere [6].
- First reaction order. Reforming reactions involve hydrocarbons and hydrogen, but due to the excess of hydrogen during reaction, its concentration is grouped together with the reaction rate coefficient.
- Pseudohomogeneous reactor model, because kinetics taken from the literature was derived under such a consideration.

2.2. Kinetics of reforming

It is well documented in the literature that at typical reforming reaction conditions the paraffins with lower carbon atoms than 5 do not undergo reaction; naphthenes with 5–12 carbon atoms are the only cycloalkanes present in naphtha so that only they are considered in the reactions. Aromatics are defined as those containing an aromatic ring and some branches thus the small compound of aromatic family is considered to be the benzene compound. Table 1 shows all considered reactions together with the kinetic rate constants at 495 K and 2170 kPa of pressure [7,8].

From the reaction steps it is possible to write a set of equations that represent the net rate of reaction for each species. For example for the pseudo-compound lumping all paraffins with seven atoms of carbon the following expression for net reaction rate is obtained:

$$r_{P7} = -0.0014 \cdot P_7 + 0.0109 \cdot P_{10} + 0.0039 \cdot P_9 + 0.0019 \cdot P_8 + 0.0020 \cdot N_7 + 0.0016 \cdot A_7, \tag{1}$$

where

P_i is the molar ratio between hydrocarbon and total molar feed in $\frac{gmol}{gmol\ Feed}$

r_{P_7} is the net reaction rate for P_7 given in $\frac{gmol\ P_7}{gmol\ Feed} \Big/ \left(\frac{hour-g\ catalyst}{g\ Feed}\right)$

That is because the amount of P_7 at any position within the reactor depends on the mass flow of naphtha (g feed/h) and the mass of catalyst (g catalyst). It is common to normalize the amount of any reactant or product by using the total feed amount in order to be able to scale up the process to any other flow-rate.

2.3. Reactor model

Instead of carrying out the material balance over a reactor volume element, for catalytic reactions is common to perform it based on a catalyst weight (catalyst weight element) contained within the reactor volume element.

The material balance under unsteady-state conditions in a catalyst weight element (Δw) is written as:

$$\Delta w\left(\frac{\varepsilon_G}{\rho_B}\right)\frac{\partial C_A}{\partial t} = u_G A_r C_A|_w - u_G A_r C_A|_{w+\Delta w} + (\overline{r'_A})\Delta w. \tag{2}$$

Dividing Eq. (2) by the catalyst weight element and taking the corresponding limit considering gas velocity (u_G) as constant:

$$\lim_{\Delta w\to 0}\frac{\varepsilon_G}{\rho_B}\frac{\partial C_A}{\partial t} = -u_G A_r \lim_{\Delta w\to 0}\frac{C_A|_{w+\Delta w} - C_A|_w}{\Delta w} + \lim_{\Delta w\to 0}(\overline{r'_A}). \tag{3}$$

The following partial differential equation is obtained:

$$\frac{\varepsilon_G}{\rho_B}\frac{\partial C_A}{\partial t} = -u_G A_r \frac{\partial C_A}{\partial w} + (r'_A). \tag{4}$$

Multiplying Eq. (4) by ρ_B/ε_G and expressing catalyst weight as the product of bed density and reactor volume ($A_r * z$), the following expression is obtained:

Table 1
Kinetic rate constants for reforming reactions (k in (g feed/h-g cat)$^{-1}$) [7].

Reaction step	Rate constant ($k \times 10^2$)
Reactions of hydrocyclization	
$P_{10} \rightarrow N_{10} + H_2$	2.54
$P_9 \rightarrow N_9 + H_2$	1.81
$P_8 \rightarrow N_8 + H_2$	1.33
$P_7 \rightarrow N_7 + H_2$	0.58
$P_6 \rightarrow N_6 + H_2$	0.00
Reactions of hydrocracking	
$P_{10} + H_2 \rightarrow P_9 + P_1$	0.49
$P_{10} + H_2 \rightarrow P_8 + P_2$	0.63
$P_{10} + H_2 \rightarrow P_7 + P_3$	1.09
$P_{10} + H_2 \rightarrow P_6 + P_4$	0.89
$P_{10} + H_2 \rightarrow 2P_5$	1.24
$P_9 + H_2 \rightarrow P_8 + P_1$	0.30
$P_9 + H_2 \rightarrow P_7 + P_2$	0.39
$P_9 + H_2 \rightarrow P_6 + P_3$	0.68
$P_9 + H_2 \rightarrow P_5 + P_4$	0.55
$P_8 + H_2 \rightarrow P_7 + P_1$	0.19
$P_8 + H_2 \rightarrow P_6 + P_2$	0.25
$P_8 + H_2 \rightarrow P_5 + P_3$	0.43
$P_8 + H_2 \rightarrow 2P_4$	0.35
$P_7 + H_2 \rightarrow P_6 + P_1$	0.14
$P_7 + H_2 \rightarrow P_5 + P_2$	0.18
$P_7 + H_2 \rightarrow P_4 + P_3$	0.32
$P_6 + H_2 \rightarrow P_5 + P_1$	0.14
$P_6 + H_2 \rightarrow P_4 + P_2$	0.18
$P_6 + H_2 \rightarrow 2P_3$	0.27
$P_5 + H_2 \rightarrow P_4 + P_1$	0.12
$P_5 + H_2 \rightarrow P_3 + P_2$	0.15
Reactions of dehydrogenation of naphthenes	
$N_{10} \rightarrow A_{10} + 3H_2$	24.50
$N_9 \rightarrow A_9 + 3H_2$	24.50
$N_8 \rightarrow A_8 + 3H_2$	21.50
$N_7 \rightarrow A_7 + 3H_2$	9.03
$N_6 \rightarrow A_6 + 3H_2$	4.02
$N_{10} + H_2 \rightarrow N_9 + P_1$	1.84
$N_{10} + H_2 \rightarrow N_8 + P_2$	1.34
$N_{10} + H_2 \rightarrow N_7 + P_3$	0.80
$N_9 + H_2 \rightarrow N_8 + P_1$	1.27
$N_9 + H_2 \rightarrow N_7 + P_2$	1.27
$N_8 + H_2 \rightarrow N_7 + P_1$	0.09
$N_{10} + H_2 \rightarrow P_{10}$	0.54
$N_9 + H_2 \rightarrow P_9$	0.54
$N_8 + H_2 \rightarrow P_8$	0.47
$N_7 + H_2 \rightarrow P_7$	0.20
$N_6 + H_2 \rightarrow P_6$	1.48
Reactions of hydrodealkylation	
$A_{10} + H_2 \rightarrow A_9 + P_1$	0.06
$A_{10} + H_2 \rightarrow A_8 + P_2$	0.06
$A_{10} + H_2 \rightarrow A_7 + P_3$	0.00
$A_9 + H_2 \rightarrow A_8 + P_1$	0.05
$A_9 + H_2 \rightarrow A_7 + P_2$	0.05
$A_8 + H_2 \rightarrow A_7 + P_1$	0.01
$A_{10} + 4H_2 \rightarrow P_{10}$	0.16
$A_9 + 4H_2 \rightarrow P_9$	0.16
$A_8 + 4H_2 \rightarrow P_8$	0.16
$A_7 + 4H_2 \rightarrow P_7$	0.16
$A_6 + 3H_2 \rightarrow N_6$	0.45

A: aromatics; N: naphthenes; P: paraffins.

$$\frac{\partial C_A}{\partial t} = -u_G A_r \frac{\rho_B}{\varepsilon_G} \frac{\partial C_A}{\partial(\rho_B A_r z)} + \frac{\rho_B}{\varepsilon_G \cdot MW_G}(r_A), \tag{5}$$

where $r_A = r_A' MW_G$.

Eq. (5) must be transformed in order to substitute the net rate of reaction of the different species in their original units. For example, by substituting the net rate of reaction for P_7, after dividing Eq. (5) by ρ_G, the following equation is found:

$$\frac{\partial P_7}{\partial t} = -\frac{u_G}{\varepsilon_G}\frac{\partial P_7}{\partial z} + \frac{\rho_B}{\varepsilon_G \rho_G MW_G} r_{P7}, \tag{6}$$

where $P_7 = C_7/\rho_G$.

For the heat balance, which is the main form of energy in packed bed catalytic reactors, the general equation reported by Mederos et al. [5] was taken, which after some simplifications leads to:

$$\left(\varepsilon_G\left(\sum C_{PGi}Y_i\right) + \frac{\varepsilon_S C_{PS}}{\rho_G}\frac{\rho_B}{1-\in_B}\right)\frac{\partial T}{\partial t} = -u_G\left(\sum C_{PGi}Y_i\right)\frac{\partial T}{\partial z} + \frac{\rho_B}{\rho_G}\frac{\sum r_i \Delta H_i}{MW_G}. \tag{7}$$

The left side of Eq. (7) accounts for heat accumulation, the first term on the right represents the convective heat and the second term on the right the heat released/consumed by chemical reaction.

$\sum C_{PGi}Y_i$ is the average heat capacity of gas.

For nomenclature of variables see the corresponding section.

Some parameters of Eqs. (6) and (7) are provided in Table 2. Other involved parameters must be calculated at reaction conditions from proper equations such as heat capacity of gases from Table 3.

In order to solve the above partial differential equation the backward finite differences method was used to discretize the partial derivatives of Y and T respect to z [9,10]. After some arrangements the material balance becomes:

$$\frac{\partial Y_i}{\partial t} = -\frac{u_G}{\varepsilon_G}\frac{Y_{i,j} - Y_{i,j-1}}{\Delta z} + \frac{\rho_B}{\varepsilon_G \rho_G MW_G} r_i, \tag{8}$$

whereas the discretized heat balance equation is found to be:

$$\left(\varepsilon_G\left(\sum CP_k Y_k\right) + \frac{\varepsilon_S C_{PS}}{C_G}\frac{\rho_B}{1-\in_B}\right)\frac{\partial T}{\partial t} = -u_G\left(\sum C_{Pk}Y_k\right)\frac{T_j - T_{j-1}}{\Delta z} + \frac{\rho_B}{C_G}\frac{\sum r_k \Delta H_k}{MW_G}. \tag{9}$$

For reactor start-up the following conditions were used:

At $t = 0$, for $0 \leqslant z \leqslant L$, $Y_i = Y_{i0}$, $T = T_0$.

At $t > 0$ for $z = L$, $\frac{\partial}{\partial z}Y_i = 0$, $\frac{\partial}{\partial z}T = 0$.

For inlet perturbation temperature the conditions are:

At $t = 0$, for $0 \leqslant z \leqslant L$, $Y_i = Y_{i\infty}$, $T = T_\infty$.

At $t > 0$ for $z = L$, $\frac{\partial}{\partial z}Y_i = 0$, $\frac{\partial}{\partial z}T = 0$.

A total of 22 differential equations were written: 20 for hydrocarbon compounds, 1 for hydrogen and 1 for the heat balance. The total length and time were divided in 100 segments in order to gain accuracy. The Matlab ODE45 solver was used to integrate the set of differential equations. To obtain profiles under steady-state the transient term was omitted. Thermodynamic properties of gas were calculated with the Peng–Robinson equation-of-state [11] and parameters involved reported in Table 2 were taken from Poling et al. [12]. Bed porosity was calculated from a correlation reported elsewhere [13]. Modified Arrhenius equation was used for correcting the rate constant by temperature and pressure effects as follows [8]:

$$k = k_{495} e^{-E_a/R\left(\frac{1}{T}-\frac{1}{495}\right)} * \left(\frac{P}{P_0}\right)^n. \tag{10}$$

The values of activation energy (E_a) and of the exponent for the effect of pressure (n) are reported in Tables 4 and 5 respectively. Reference pressure was 2170 kPa while reaction pressure is fixed according to the industrial operation.

Dynamic modeling of the entire configuration of the catalytic reforming process is not an easy task, since it includes a series of three or four fixed-bed reactors with heat exchangers placed between them. The difficulty for modeling such a study comes from the fact that at start-up conditions the feed passes through the first reactor, and then its temperature is raised at the same value of that at the inlet of the first reactor to be further fed to the second reactor. This operation is repeated as many times as the number of reactors. Dynamic modeling of this in series reactor-heat exchanger arrangement requires more computing time and programming efforts. That is why in this contribution, as first attempt, only one reactor is modeled to simplify the calculations.

Table 2
Some parameters for Eqs. (8) and (9).

Parameter	Value
ε_G	0.39 cm^3_G/cm^3_r
$\in_B$	0.39 cm^3_G/cm^3_r
ρ_B	0.40 g cat/cm^3_r
MW_G	109.5 g/gmol
ρ_G	6.56×10^{-4} gmol/cm^3
$u_{G'}$	4.33×10^4 (cm^3_G/cm^3_r) (cm_r/h)
C_{PS}	1.1497 cal/g
ε_S	0.69 cm^3_S/cm^3_r

Table 3
Thermodynamic properties of selected hydrocarbons.

Component	$Cp = A + B * T + C * T^2 + D * T^3 + E * T^4$ in J/gmol-K; T in K					MW	ΔH	T_c	P_c	ω
	A	B	C	D	E	g/gmol	J/gmol	K	Bar	–
A_{10}	6.49E + 00	1.91E−02	1.57E−04	−2.21E−07	8.89E−11	134.221	−2.03E + 04	6.50E + 02	3.05E + 01	3.83E−01
A_9	5.10E + 00	1.74E−02	1.36E−04	−1.93E−07	7.82E−11	120.194	−2.05E + 03	6.40E + 02	3.22E + 01	3.64E−01
A_8	4.54E + 00	1.06E−02	1.36E−04	−1.93E−07	7.89E−11	106.167	2.99E + 04	6.17E + 02	3.61E + 01	3.04E−01
A_7	3.87E + 00	3.56E−03	1.34E−04	−1.87E−07	7.69E−11	92.141	5.02E + 04	5.92E + 02	4.11E + 01	2.64E−01
A_6	3.55E + 00	−6.18E−03	1.44E−04	−1.98E−07	8.23E−11	78.114	8.29E + 04	5.62E + 02	4.90E + 01	2.10E−01
N_{10}	−7.26E + 00	1.28E−01	−7.07E−05	1.35E−08	0.00E + 00	140.26	−2.13E + 05	6.67E + 02	3.15E + 01	3.62E−01
N_9	−7.22E + 00	1.13E−01	5.63E−05	8.21E−09	0.00E + 00	126.243	−2.07E + 05	6.40E + 02	2.83E + 01	2.37E−01
N_8	−7.23E + 00	1.04E−01	−5.58E−05	9.99E−09	0.00E + 00	112.215	−1.72E + 05	6.47E + 02	3.57E + 01	2.54E−01
N_7	3.15E + 00	1.84E−02	1.36E−04	−1.87E−07	7.36E−11	98.188	−1.55E + 05	5.72E + 02	3.47E + 01	2.35E−01
N_6	4.04E + 00	−4.43E−03	1.68E−04	−2.08E−07	7.75E−11	84.161	−1.23E + 05	5.54E + 02	4.07E + 01	2.11E−01
P_{10}	1.35E + 01	4.14E−03	2.31E−04	−3.05E−07	1.20E−10	142.285	−2.50E + 05	6.18E + 02	2.11E + 01	4.90E−01
P_9	1.22E + 01	4.58E−03	2.04E−04	−2.68E−07	1.05E−10	128.258	−2.29E + 05	5.95E + 02	2.29E + 01	4.45E−01
P_8	1.08E + 01	4.98E−03	1.78E−04	−2.31E−07	8.98E−11	114.231	−2.09E + 05	5.69E + 02	2.49E + 01	3.99E−01
P_7	9.63E + 00	4.16E−03	1.55E−04	−2.01E−07	7.77E−11	100.204	−1.88E + 05	5.40E + 02	2.74E + 01	3.50E−01
P_6	8.83E + 00	−1.66E−04	1.43E−04	−1.83E−07	7.12E−11	86.177	−1.67E + 05	5.08E + 02	3.03E + 01	3.00E−01
P_5	7.55E + 00	−3.68E−04	1.18E−04	−1.49E−07	5.75E−11	72.15	−1.47E + 05	4.70E + 02	3.37E + 01	2.52E−01
P_4	5.55E + 00	5.54E−03	8.06E−05	−1.06E−07	4.13E−11	58.123	−1.26E + 05	4.25E + 02	3.80E + 01	2.00E−01
P_3	3.85E + 00	5.13E−03	6.01E−05	−7.89E−08	3.08E−11	44.097	−1.05E + 05	3.70E + 02	4.25E + 01	1.52E−01
P_2	4.18E + 00	−4.43E−03	5.66E−05	−6.65E−08	2.49E−11	30.07	−8.38E + 04	3.05E + 02	4.87E + 01	9.90E−02
P_1	4.57E + 00	−8.98E−03	3.63E−05	−3.41E−08	1.09E−11	16.043	−7.45E + 04	1.91E + 02	4.60E + 01	1.10E−02
H_2	2.88E + 00	3.68E−03	−7.72E−06	6.92E−09	8.23E−11	2.016	0.00E + 00	3.30E + 01	1.29E + 01	−2.17E−01

C_P: heat capacity; MW: molecular weight; ΔH: enthalpy; T_c: critical temperature; P_c: critical pressure; ω: acentric factor.

Table 4
Activation energies for different reforming reactions [16].

Reaction		E_a (kcal/mol)
Dehydrocyclization of paraffins	$(P_n \rightarrow N_n)$	45
Hydrocracking of paraffins	$(P_n \rightarrow P_{n-i} + P_i)$	55
Dehydrogenation of naphthenes	$(N_n \rightarrow A_n)$	30
Hydrodealkylation of naphthenes	$(N_n \rightarrow N_{n-i} + P_i)$	55
Ring opening of naphthenes	$(N_n \rightarrow P_n)$	45
Hydrodealkylation of aromatics	$(A_n \rightarrow A_{n-i} + P_i)$	40
Ring opening of aromatics	$(A_n \rightarrow P_n)$	45
Hydrogenation of aromatics	$(A_n \rightarrow N_n)$	30

Table 5
Exponents for Eq. (10) [17].

Reaction	n
Hydrocracking of paraffins	0.433
Dehydrocyclization of paraffins	−0.700
Dehydrogenation/hydrogenation of aromatics	0.000
Hydrodealkylation of aromatics and naphthenes	0.500
Other reactions	0.000

3. Results and discussion

The following operating conditions were used for the simulation: base temperature of the feed of 490 °C, pressure of 3446 kPa and 198.7 m^3/h of naphtha flowrate with 730 kg/m^3 liquid density. The composition of the feed is reported in Table 6. Other conditions and characteristics of the system are reported elsewhere [2]. Reactor dimensions are: length of 4.9 m and diameter of 2.4 m.

Paraffins with 1–10 carbon atoms range were used for representing the linear hydrocarbons chains. Normal alkanes were selected for such a purpose. Because naphthenic and aromatics exhibit different standard formation heats depending on structure, in order to avoid excessive computation only those that follow a linear or almost linear relationship between carbon number and standard formation enthalpy were chosen as depicted in Fig. 1.

Fig. 2 shows the dynamic profiles of P_{10} pseudo-compound as function of dimensionless catalytic length. At short times very low concentration of that compound within the reactor is observed; as time increases a well-defined decreasing profile

Table 6
Feed composition.

Compound	Mol%
P_{10}	7.79
P_9	10.34
P_8	13.93
P_7	14.86
P_6	10.77
P_5	0.94
N_{10}	1.23
N_9	4.17
N_8	4.62
N_7	5.55
N_6	4.25
A_{10}	3.4
A_9	5.52
A_8	7.13
A_7	3.68
A_6	1.82

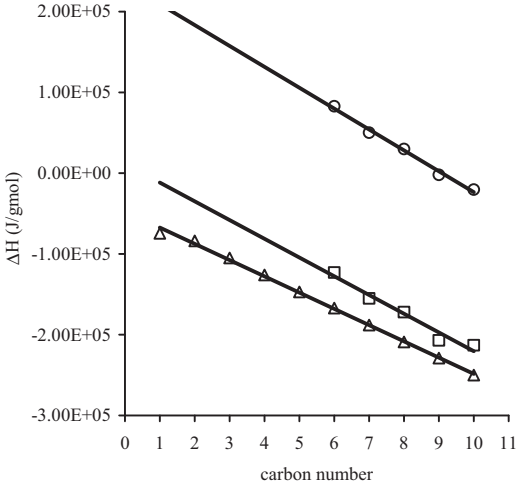

Fig. 1. Relationship between carbon number and standard heat of formation for different hydrocarbon families: (△) Paraffins, (□) Naphthenes, (○) Aromatics.

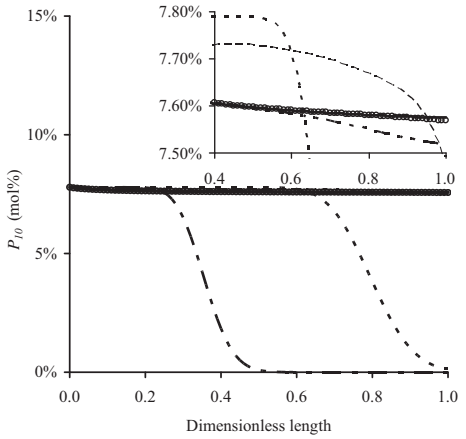

Fig. 2. Concentration profiles of P_{10} compound as function of dimensionless catalytic bed length and time: (– – –) 0.25 h, (– – – –) 0.50 h, (– – –) 0.75 h, (– – – –) 1.25 h, (⋯⋯⋯) 2.00 h, (———) Steady-state.

is developed. For practical purposes at 2 h it is assumed the quasi steady-state. In order to better appreciate the profile at quasi steady-state and steady-state solution a zoom window was used for the zone when the curves are indistinguishable. Even with this artifice the differences between developed profiles at 2 h and steady-state were not evident.

Lower molecular weight paraffins are expected to be increased in concentration along the reactor and with time because they are produced from hydrocracking of longer paraffins and aromatic dealkylation mainly while they do not produce lower molecular chains. For instance P_5 dynamic profiles are shown in Fig. 3 from which the expected profile is confirmed. Similarly to P_{10} profile at 2 h P_5 concentration was closer to that of the steady-state overlapping these two curves.

In Fig. 4 N_9 concentration profiles are depicted as function of time and dimensionless axial position of reactor. The heavy molecular compound exhibits a net diminution concentration at steady state and only increases its concentration with time, that is because naphthenic compounds are the main species that undergo disappearance allowing for upgrading the octane number of the reacting mixture.

A_9 aromatic compound profiles as function of dimensionless reactor length and time are shown in Fig. 5. It is observed that in some time range A_9 concentrations are higher than those at steady-state.

Developed profiles of reactor temperature as function of dimensionless length and time are shown in Fig. 6. Temperature dynamic profiles are spread more widely as compared with concentration profiles at the same selected times. At short times the reactor temperature remains high so that reaction rates occur rapidly provoking a maximum concentration within the reactor of those compounds that are directly linked with the fastest reactions as in the case of aromatics yield.

The times to reach the quasi steady-state outlet reactor concentration of the above analyzed compound profiles are compared in Fig. 7. It is observed that A_9 and P_5 pseudo-compounds exhibit a maximum outlet concentration at near 0.7 h while the concentration of the other pseudo-compounds still exhibits an increase. As can be seen from these profiles different times are necessary to reach the quasi steady-state at the outlet reactor position for different compounds, for example aromatic compounds require approximately 1 h to reach such a condition whereas for naphthenic compound almost 2 h are necessary for achieving quasi steady-state. This can be explained by the fact that the compounds exhibit different reaction rates and because the network of reaction is complex, thus affecting the response to transients in different way.

In Fig. 8 it is observed that catalytic reforming is a net endothermic process, that is endothermic character predominates over exothermic because the reaction needs heat from the environment (positive values) all times along the bed.

In Fig. 9 the profile of outlet reactor temperature is shown. It is observed that the exit reactor temperature is always equal or lower of that at the inlet. At short times (lower than 0.5 h) the temperature reactor remains almost constant (and similar to the feed temperature – dotted line-) due to the highest concentration of reactants is closer to the reactor entrance and changes in temperature are minimal at the reactor outlet. As reactants pass through the reactor as time increases large changes in reactor temperature are observed. At longer times slow rate of temperature variation is observed that still provokes significant variation in rates of reaction with higher activation energies and hence in concentration profiles.

Fig. 10 reports hydrogen concentration as function of time and reactor position. As a result of dehydrogenation reactions H_2 is produced reaching a maximum in concentration at different times depending on the bed position. This figure can be used for optimizing the hydrogen production because it allows for identifying the time when hydrogen production is maximum and hence a policy of removing hydrogen can be followed.

In some literature papers dealing with dynamic reactor modeling where several reactions were studied only characteristic time interval of transient behavior for one reaction was reported [14,15]. In those works it was presumed that the most important reaction governs the characteristic times and in consequence it was used for simulation purposes. In this study the maximum time to reach the quasi steady-state among those of several compounds was chosen as characteristic time to

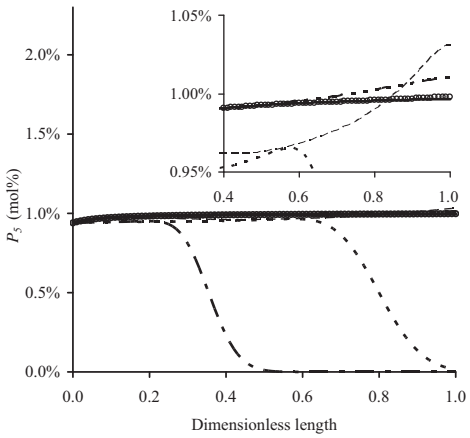

Fig. 3. Concentration profiles of P_5 as function of dimensionless catalytic bed length and time: (– – –) 0.25 h, (– – – –) 0.50 h, (– – –) 0.75 h, (– – – –) 1.25 h, (∞∞∞∞∞∞∞∞∞∞) 2.00 h, (———) Steady-state.

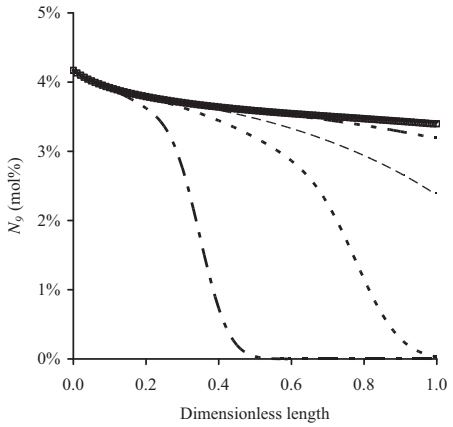

Fig. 4. Concentration profiles of N_9 as function of dimensionless catalytic bed and time: (– – –) 0.25 h, (- - - - -) 0.50 h, (– – –) 0.75 h, (– – – –) 1.25 h, (⟿) 2.00 h, (——) Steady-state.

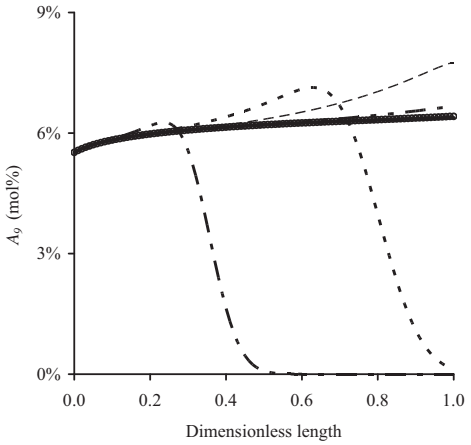

Fig. 5. Concentration profiles of A_9 as function of dimensionless catalytic bed and time: (– – –) 0.25 h, (- - - - -) 0.50 h, (– – –) 0.75 h, (– – – –) 1.25 h, (⟿) 2.00 h, (——) Steady-state.

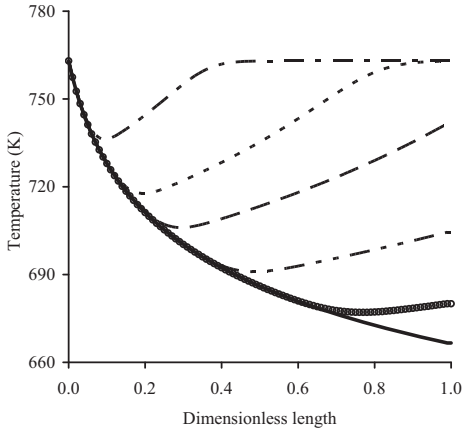

Fig. 6. Profiles of temperature within the reactor as function of dimensionless catalytic bed and time: (– – –) 0.25 h, (- - - - -) 0.50 h, (– – –) 0.75 h, (– – – –) 1.25 h, (⟿) 2.00 h, (——) Steady-state.

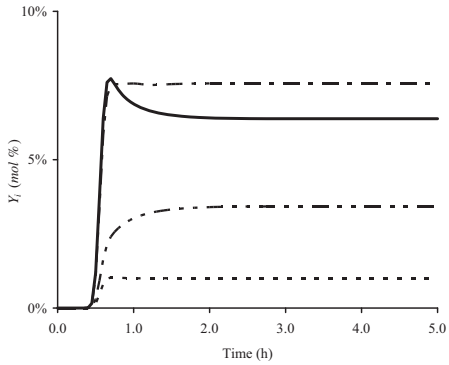

Fig. 7. Outlet composition of several compounds as function of time. (– – –) P_5; (– – –) P_{10}; (– – – –) N_9; (——) A_9.

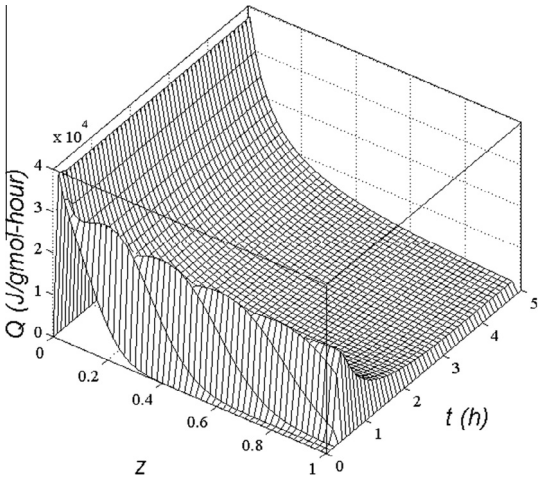

Fig. 8. Rate of heat production due to chemical reaction.

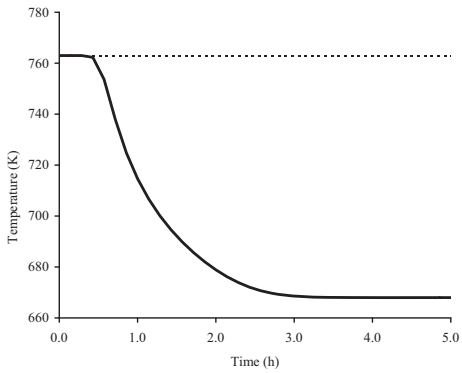

Fig. 9. Outlet reactor temperature as function of time.

attain such a condition. Based on Figs. 7 and 8 it can be concluded that almost 3 h are necessary to attain the quasi steady-state.

In order to observe the response to perturbations in the compound profiles and temperature by varying the inlet temperature such a variable was increased/decreased in 10 K respect to its original value. In Fig. 11 the profiles of N_9 are shown for a 10 K decrease in inlet temperature. It is observed that the main differences with steady-state profile occur in the middle and at reactor outlet positions. Near the reactor entrance no remarkable differences are observed because at this position high reaction rate of N_9 is conserved due to high reactant concentration.

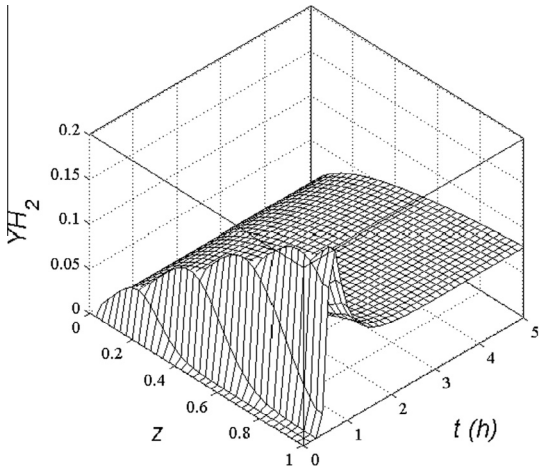

Fig. 10. Hydrogen production as function of time and dimensionless reactor length.

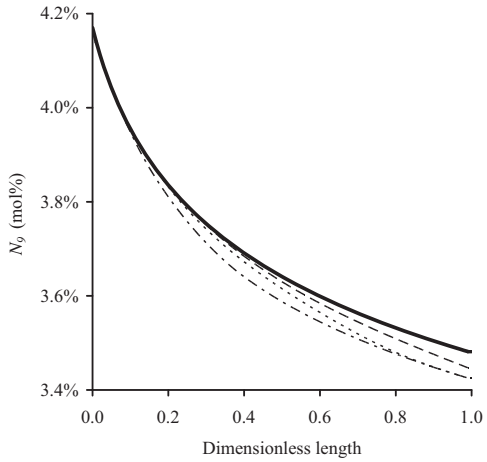

Fig. 11. Perturbed profiles of N_9 due to change in inlet temperature (T_0 = 753 K). (– – –) 0.05 h; (– – – –) 0.10 h; (– – –) 0.15 h; (——) Steady-state (T_0 = 763 K).

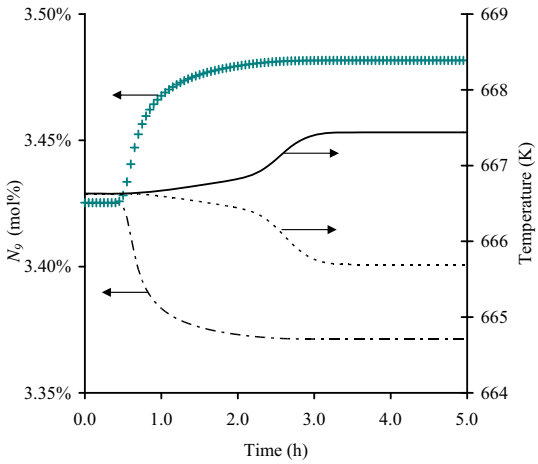

Fig. 12. Perturbed profiles of N_9 and temperature at the exit reactor position due to change in inlet temperature. N_9: (+++) at T_0 = 773 K; (——) at T_0 = 763 K; Temperature: (– – – –) T_0 = 763 K; (– – –) T_0 = 773 K.

In Fig. 12 the outlet reactor compositions of N_9 and temperature are plotted as function of inlet temperature and time. When the inlet reactor temperature was higher than the reference (490 °C) the concentration of product was also higher and vice versa, that is because the temperature affects directly the reaction rate and thus the naphthenes consumption. Similar behavior was observed for temperature at the outlet reactor position. The time required to attain the quasi steady-state for reactant concentration was similar in both conditions of perturbations. The time to reach the quasi steady-state was higher for temperature than for N_9 concentration. Comparing the time to reach the quasi steady-state from start-up and perturbation-temperature conditions it is observed that they are almost similar.

4. Conclusions

Dynamic modeling of the reactor used for catalytic reforming of naphtha was carried out by using material and heat balances. By means of simulation two transient conditions were studied: the start-up and temperature inlet perturbations. Similar time to attain the quasi steady-state was observed under these two operating conditions. It was found that the temperature requires more time to reach the quasi steady-state than concentration of any compound.

References

[1] G.J. Antos, A.M. Aitani, Catalytic Naphtha Reforming, second ed., Marcel Dekker Inc., New York, 2004.
[2] M.A. Rodriguez, J. Ancheyta, Detailed description of kinetic and reactor modeling for naphtha catalytic reforming, Fuel 90 (2011) 3492–3508.
[3] J. Ancheyta, E. Villafuerte, L. García, E. González, Modeling and simulation of four catalytic reactors in series for naphtha reforming, Energy Fuels 15 (2001) 887–893.
[4] R. Sotelo, G.F. Froment, Fundamental kinetic modeling of catalytic reforming, Ind. Eng. Chem. Res. 48 (2009) 1107–1119.
[5] F. Mederos, I. Elizalde, J. Ancheyta, Steady-state and dynamic reactor models for hydrotreatment of oil fractions: a review, Rev. Sci. Eng. 51 (2009) 485–607.
[6] G.F. Froment, K.B. Bischoff, Chemical Reactor Analysis and Design, second ed., Wiley, USA, 1990.
[7] H.G. Krane, A.B. Groh, B.D. Shulman, J.H. Sinfeit, Reactions in catalytic reforming of naphthas, in: Proceedings of the Fifth World Petroleum Congress, May 30, 1959, pp. 39–51 [Sec. III].
[8] J. Ancheyta, R.E. Aguilar, New model accurately predicts reformate composition, Oil Gas J. (Jan. 31, 1994) 93–95.
[9] I. Ingham, I.J. Dunn, E. Heinzle, J.E. Prenosil, J.B. Snape, Chemical Engineering Dynamics: An Introduction to Modeling and Computer Simulation, third ed., Wiley VCH, Germany, 2007.
[10] W.E. Schiesser, The Numerical Method of Lines-integration of Partial Differential Equations, Academic Press Inc., USA, 1991.
[11] D.Y. Peng, D.B. Robinson, A new two-constant equation of state, Ind. Eng. Chem. Fundam. 15 (1976) 59–64.
[12] E.B. Poling, J.M. Prausnitz, J.P. O'Connel, The properties of gases and liquids, McGraw-Hill, New York, 2001. 865 pp.
[13] F. Benyahia, K.E. ÓNeill, Enhanced voidage correlation for packed beds of various particles shapes and sizes, Part. Sci. Technol. 23 (2005) 169–177.
[14] F.S. Mederos, M.A. Rodríguez, J. Ancheyta, E. Arce, Dynamic modeling and simulation of catalytic hydrotreating reactors, Energy Fuels 20 (2006) 936–945.
[15] F.S. Mederos, J. Ancheyta, I. Elizalde, Dynamic modeling and simulation of hydrotreating of gas oil obtained from heavy crude oil, Appl. Catal. A 425–426 (2012) 13–27.
[16] J. Henningsen, M. Bundgaard-Nielson, Catalytic reforming, Brit. Chem. Eng. 15 (1970) 1433–1436.
[17] J.H. Jenkins, T.W. Stephens, Kinetics of cat reforming, Hydrocarbon Process. (November, 1980).